MRI of the Brachial Plexus: Modified Imaging Technique Leading to a Better Characterization of Its Anatomy and Pathology

CARLOS TORRES[1], KATHLEEN MAILLEY[2], RAQUEL DEL CARPIO O'DONOVAN[3]

[1] Department of Diagnostic Imaging, Neuroradiology Section, University of Ottawa, The Ottawa Hospital Civic and General Campus; Ottawa, Ontario, Canada
[2] Department of Diagnostic Imaging, The Montreal General Hospital; Montreal, Quebec, Canada
[3] McGill University Health Centre, Department of Diagnostic Imaging, Neuroradiology Section, The Montreal General Hospital; Montreal, Quebec, Canada

Key words: magnetic resonance imaging, brachial plexus, diagnosis, modified technique, anatomy, pathology

SUMMARY – *Magnetic resonance imaging (MRI) is the imaging modality of choice for the evaluation of the brachial plexus due to its superior soft tissue resolution and multiplanar capabilities. The evaluation of the brachial plexus however represents a diagnostic challenge for the clinician and the radiologist. The imaging assessment of the brachial plexus, in particular, has been traditionally challenging due to the complexity of its anatomy, its distribution in space and due to technical factors. Herein, we describe a modified technique used in our institution for the evaluation of the brachial plexus which led to a substantial decrease in scanning time and to better visualization of all the segments of the brachial plexus from the roots to the branches, in only one or two images, facilitating therefore the understanding of the anatomy and the interpretation of the study. To our knowledge, we are the first group to describe this technique of imaging the brachial plexus. We illustrate the benefit of this modified technique with an example of a patient with a lesion in the proximal branches of the left brachial plexus that was clinically suspected but missed on conventional brachial plexus imaging for six consecutive years. In addition, we review the common and infrequent benign and malignant pathology that can affect the brachial plexus.*

Introduction

The brachial plexus is a major neural structure that provides sensory and motor innervation to the upper extremity. Different imaging modalities can be used to study the brachial plexus, including magnetic resonance imaging (MRI), computed tomography (CT) and ultrasound (US) [1], however MRI is the imaging modality of choice for the evaluation of the brachial plexus due to its superior soft tissue resolution and multiplanar capabilities [1-4]. There is a wide range of disease processes that can involve the brachial plexus including primary and secondary tumors, radiation fibrosis, trauma and inflammatory processes. Clinically, a brachial plexopathy represents a diagnostic challenge as the symptoms are often non-specific and adequate localization of lesions along the course of the plexus is difficult. Although electromyography can help clarify whether a lesion is central (preganglionic) or peripheral (postganglionic) based on the pattern of involvement of the plexus, it is not useful for a more exact localization [1]. MR imaging plays an essential role in differentiating preganglionic injuries from postganglionic lesions, a differentiation that is crucial for determining the management of brachial plexus injury, predominantly in the setting of trauma.

The imaging assessment of the brachial plexus, however, has been traditionally challenging due to the complexity of its anatomy

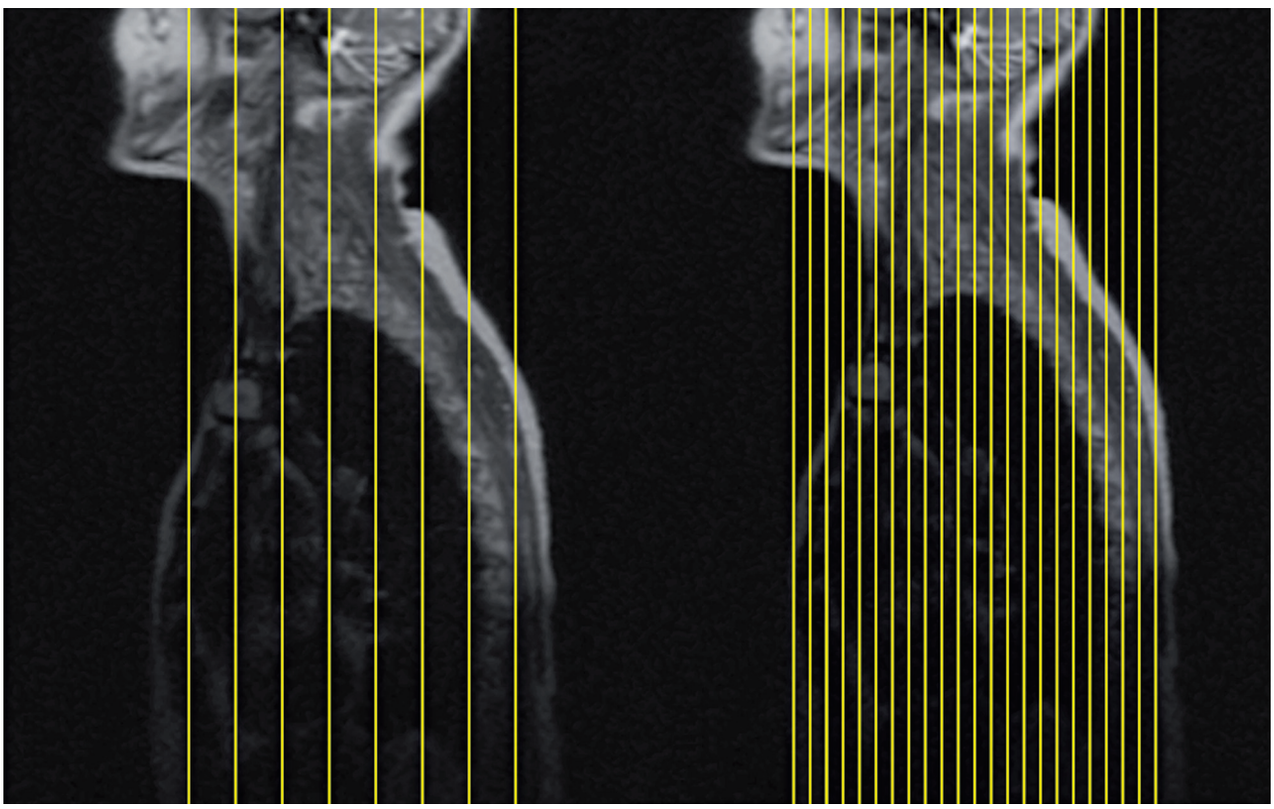

A B

Figure 1 The number of slices in the localizer sequence has been increased to improve visualization of the nerve roots. Conventional localizer (A), modified localizer (B).

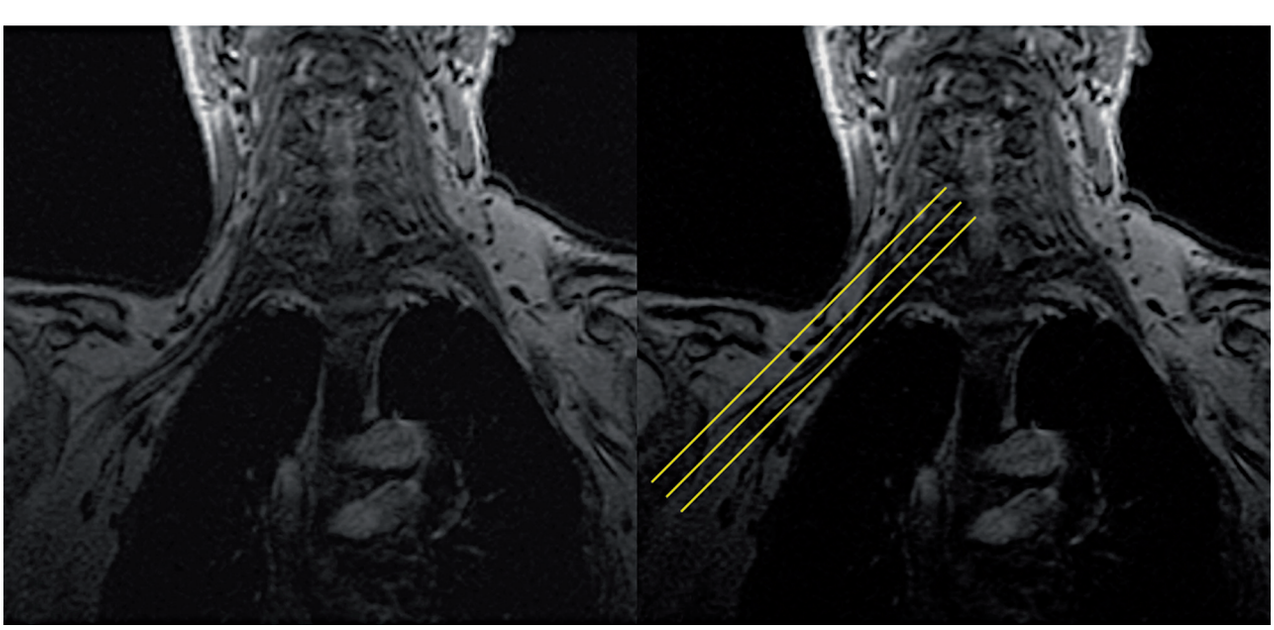

A B

Figure 2 Note the improved visualization of the right brachial plexus (A) in the coronal localizer which enables the axial oblique images to be planned angling parallel to the nerve roots (b).

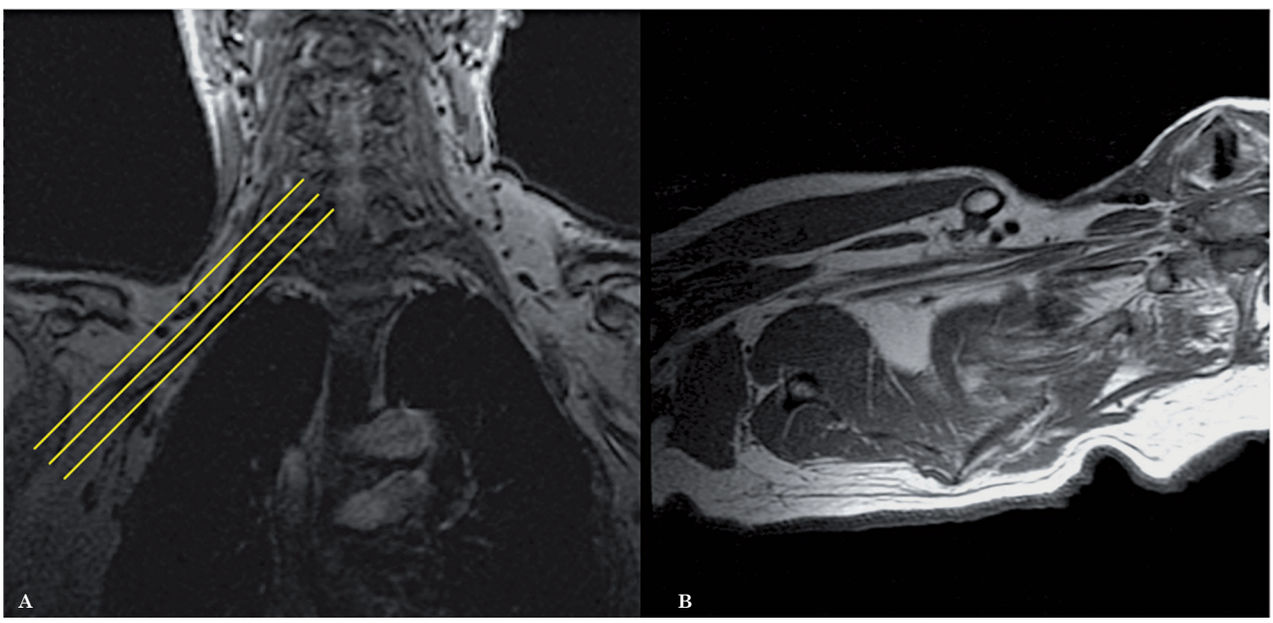

Figure 3 Axial oblique images are planned from the coronal localizer in the planes of the trunks and divisions of the brachial plexus (A). The images obtained allow the roots, trunks, divisions and cords to be assessed in only 1 to 2 slices (B).

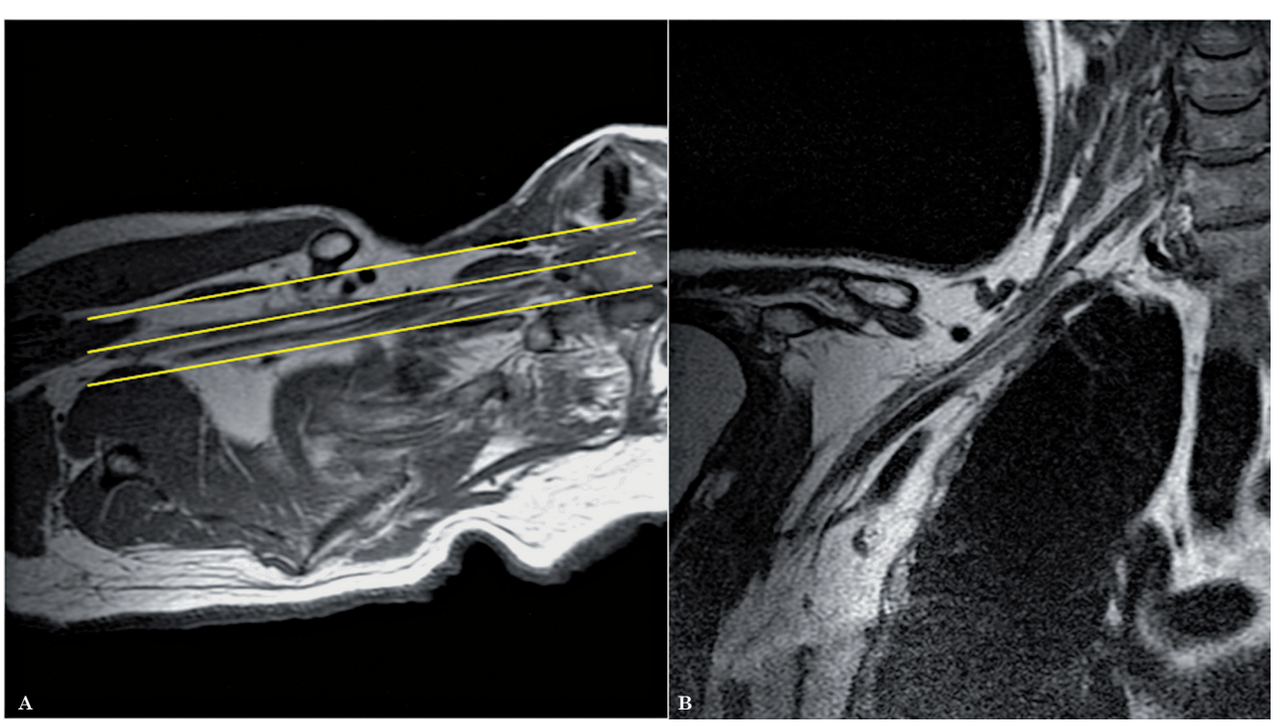

Figure 4 Coronal oblique images are planned from the axial oblique dataset, also following the plane of the proximal and mid segments of the brachial plexus (A). The images obtained demonstrate in a single slice, the roots, trunks, divisions and cords (B).

and distribution in space. Another important limitation is the prolonged scanning time the patients have to endure. This is particularly problematic in the clinical setting of trauma or neoplastic involvement of the plexus since the patients are in pain and therefore move during the study, resulting in inadequate images for interpretation.

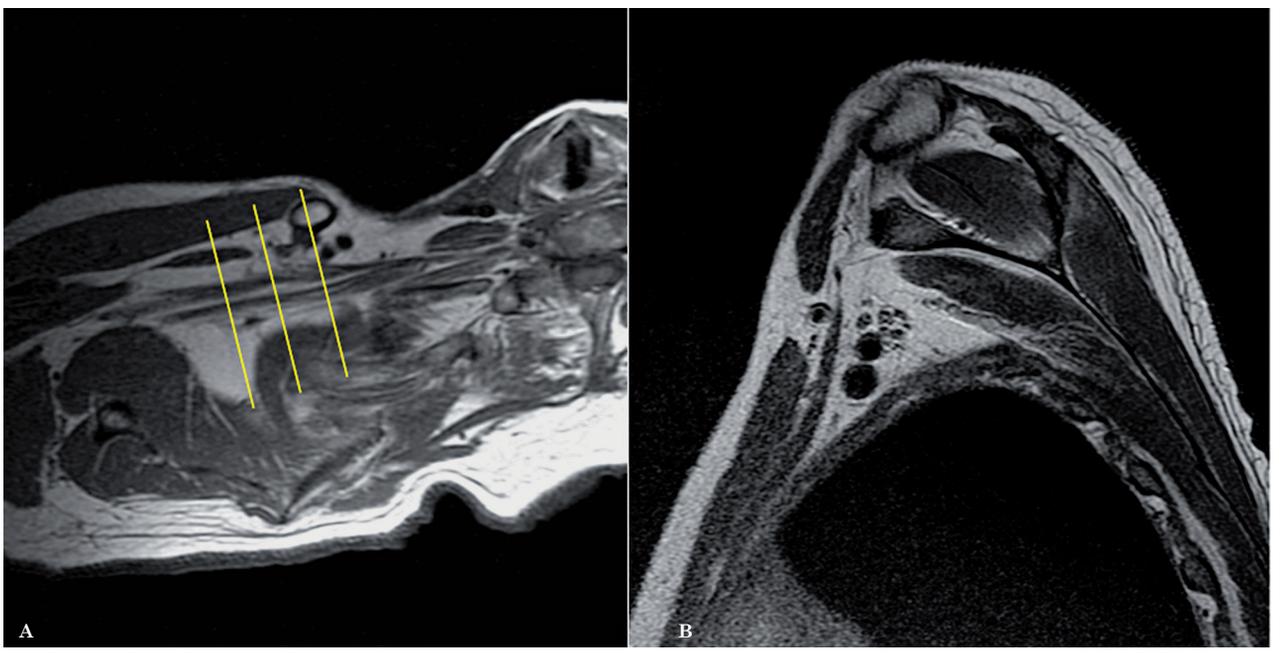

Figure 5 Sagittal oblique images are also planned from the axial oblique dataset, perpendicular to the mid segment of the brachial plexus (A,B).

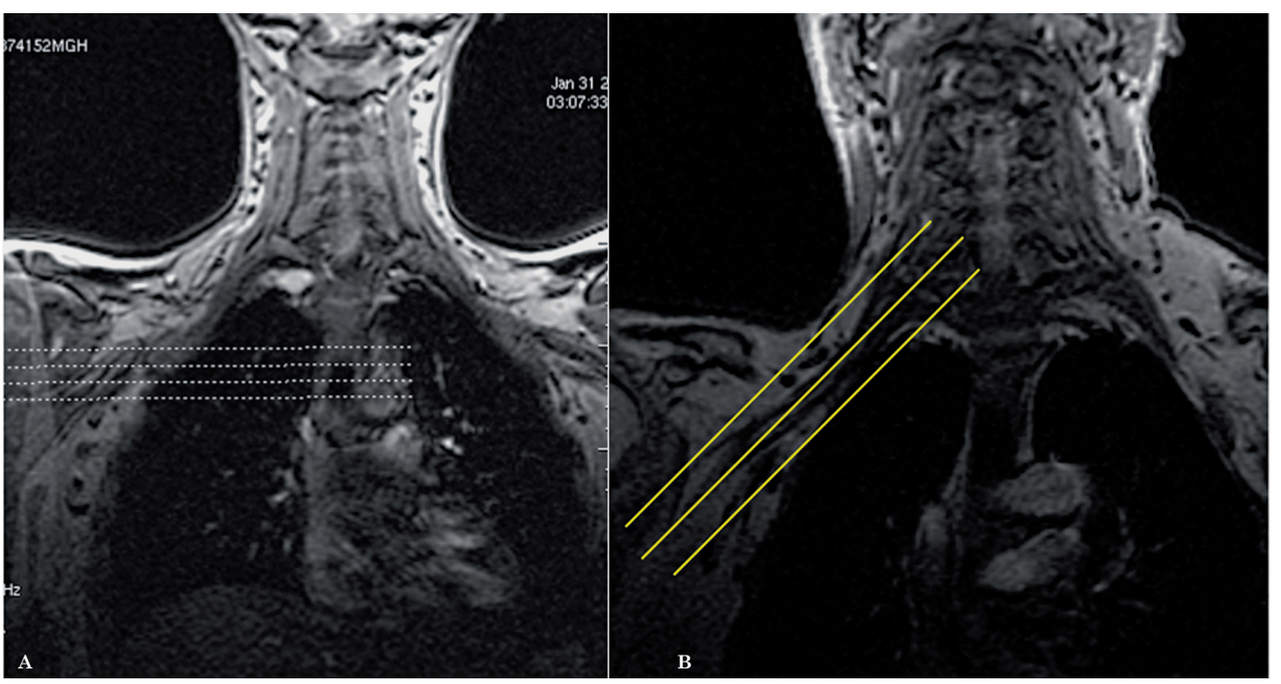

Figure 6 Planning of axial images: Conventional technique (A) and Modified technique (B).

Given our institution is a referral center for trauma and oncology patients, we found a solution to decrease the amount of time a patient spends in the magnet by modifying the way we image the brachial plexus without compromising the diagnostic quality of the study. Herein, we describe the protocol that we use at our institution for the evaluation of the brachial plexus, illus-

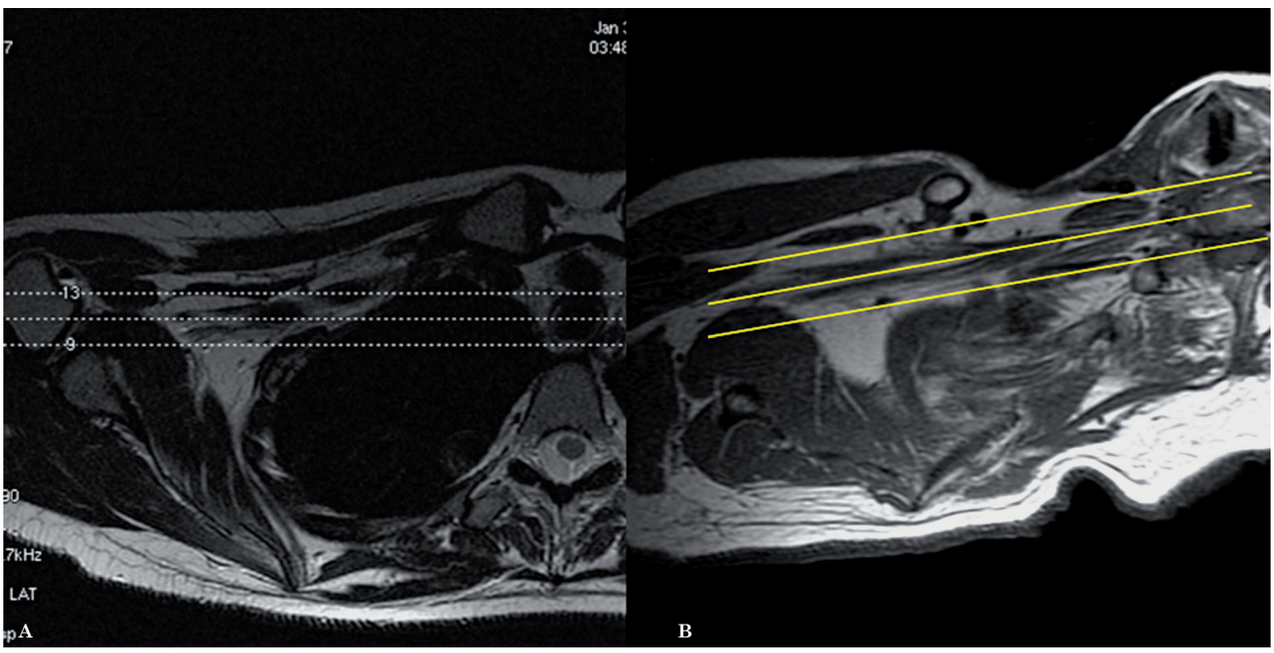

Figure 7 Planning of coronal images: Conventional technique (A) and Modified technique (B).

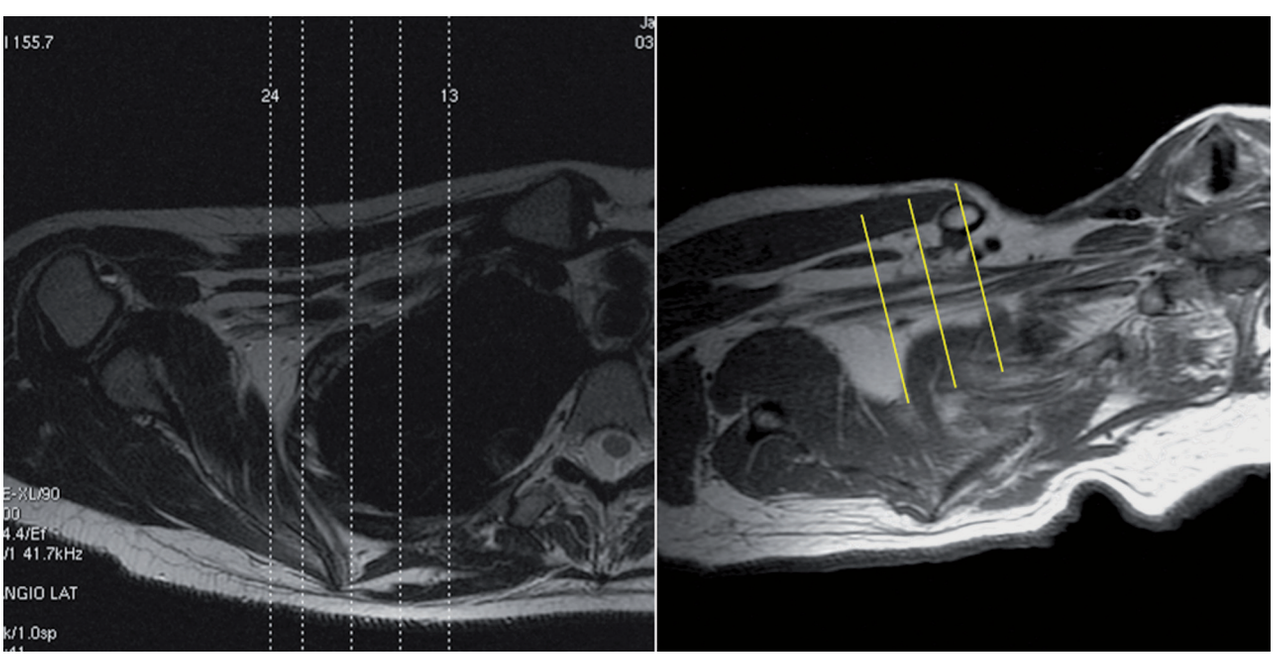

A B

Figure 8 Planning of sagittal images: Conventional technique (A) and Modified technique (B).

trating the normal anatomy and the benefits of using this modified technique. As an unexpected result, we were able to visualize and follow all the segments of the brachial plexus from the roots to the branches in only one or two images, facilitating the understanding of the anatomy and the interpretation of the study. To our knowledge, we are the first group to describe this technique

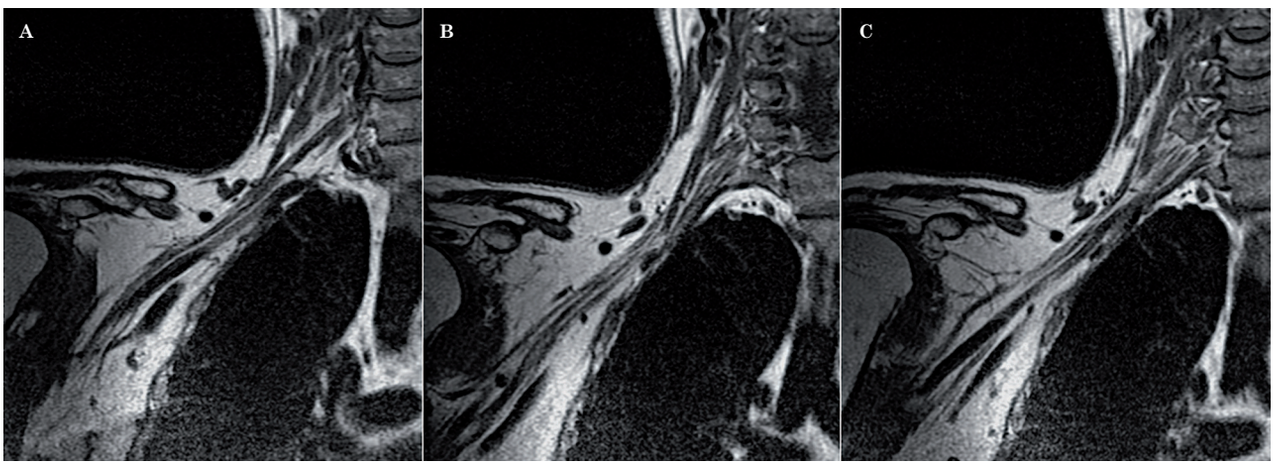

Figure 9 Normal anatomy of the brachial plexus. Coronal oblique images allow the roots, trunks, divisions, cords and branches to be assessed in a continuous fashion in 1 to 3 slices (A-C).

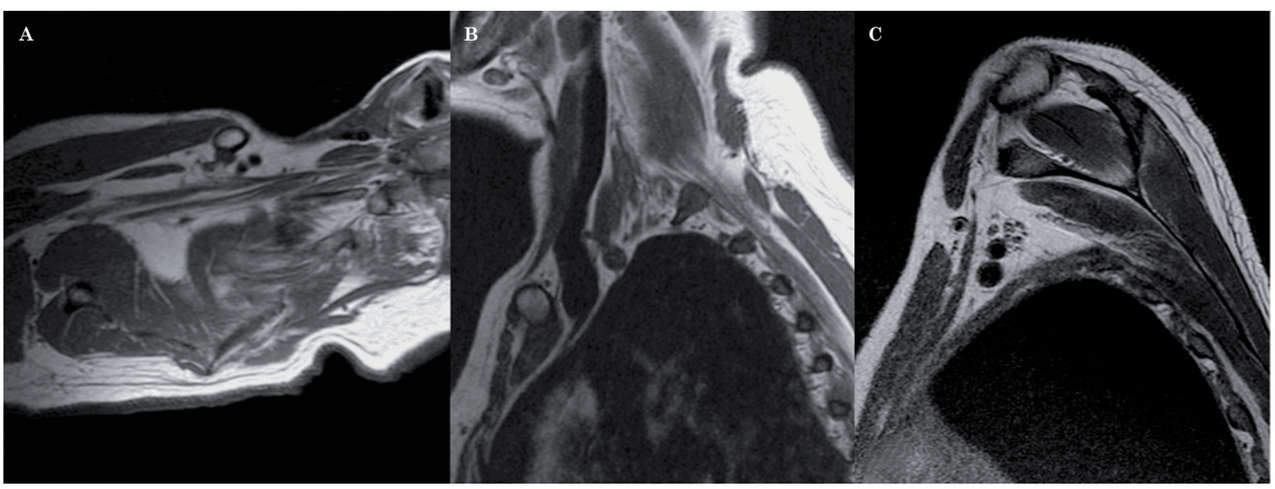

Figure 10 Normal anatomy of the brachial plexus. A T1-weighted sequence in the axial oblique plane (A) shows the roots, the trunks and the divisions of the brachial plexus in a continuous fashion, surrounded by fat. Sagittal oblique T1-weighted images demonstrate the roots within the scalene triangle (B) and the cords in the axillary region (C).

of imaging the brachial plexus. We illustrate the benefit of this modified technique with an example of a patient with a lesion in the proximal branches of the left brachial plexus that was clinically suspected but missed on conventional brachial plexus imaging for six consecutive years.

Imaging Protocol and Technique

MR protocol parameters

All the patients are scanned on a 1.5 Tesla system (Twinspeed Excite HD, General Electric) using the eight-channel neurovascular coil. Our standard protocol includes a three-plane localizer followed by T1W FSE (TR/TE: 500/10, FOV:22-28 cm, matrix : 320×224 mm) in the axial oblique, coronal oblique and sagittal oblique planes, a T2W FSE sequence (TR/TE: 4000/110), FOV: 22-28 cm, matrix: 384×256 mm) in the axial oblique plane, and a coronal T2 FSE STIR sequence to suppress the fat signal. The slice thickness is 3 mm with a 1mm interslice gap. Gadolinium is not routinely used and could be added to better characterize a neoplastic process. When the comparison between the symptomatic and the normal side is necessary, images with a larger field of view (FOV) could be obtained in order to include the bilat-

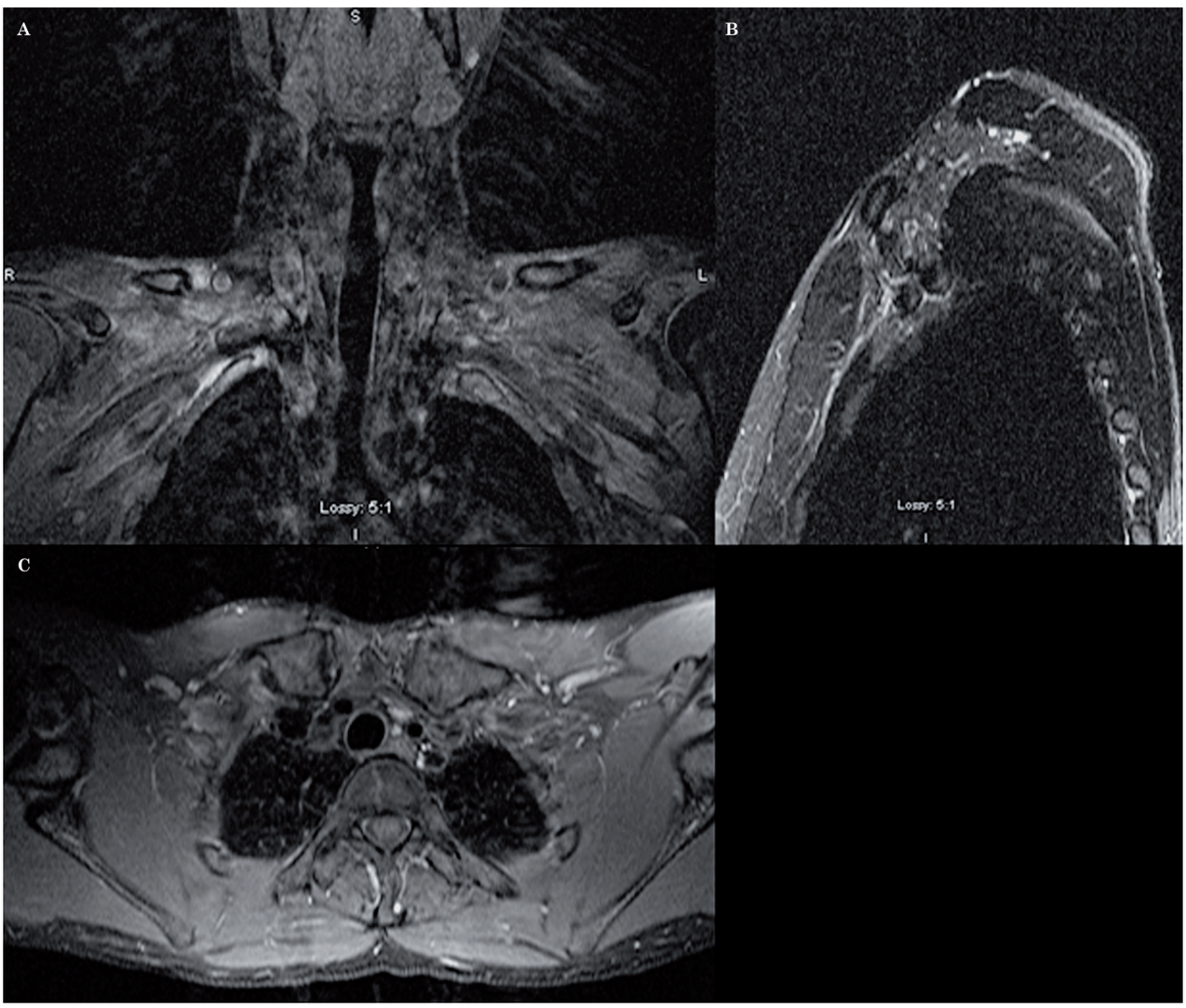

Figure 11 MRI of the left brachial plexus using the Conventional technique, in 2005, for the study of ulnar neuropathy. Coronal T1-weighted sequence post-contrast with fat saturation (A), sagittal STIR (B) and axial T1-weighted sequence post-contrast with fat saturation (C). No abnormality was identified.

eral brachial plexus, using a body coil. A similar protocol could be obtained in a 3T system using a surface coil, without interslice gap.

Due to the complex anatomy of the brachial plexus, it is difficult to follow its segments in a continuous fashion on the true axial and true coronal images when using the conventional technique. Since the brachial plexus runs obliquely from superomedial to inferolateral in the coronal plane [3], we decided to acquire axial oblique and coronal oblique images instead. In order to do that, we increased the number of slices in the coronal localizer (Figure 1) which allowed us to better identify the segments of the brachial plexus in that plane (Figure 2).

We subsequently planned the axial images from the localizer, with an angulation parallel to the trunks and divisions of the brachial plexus. The result being that instead of true axial images, we obtained axial oblique images (Figure 3). The coronal images are then planned from the axial oblique images using an angle parallel to the proximal and mid brachial plexus (Figure 4). Finally, the sagittal images are planned from the axial oblique dataset, perpendicular to the mid segment of the brachial plexus (Figure 5). By planning the images in an oblique fashion, following the course of the segments of the brachial plexus, the heart and lungs are avoided, thus reducing motion artefacts and eliminating

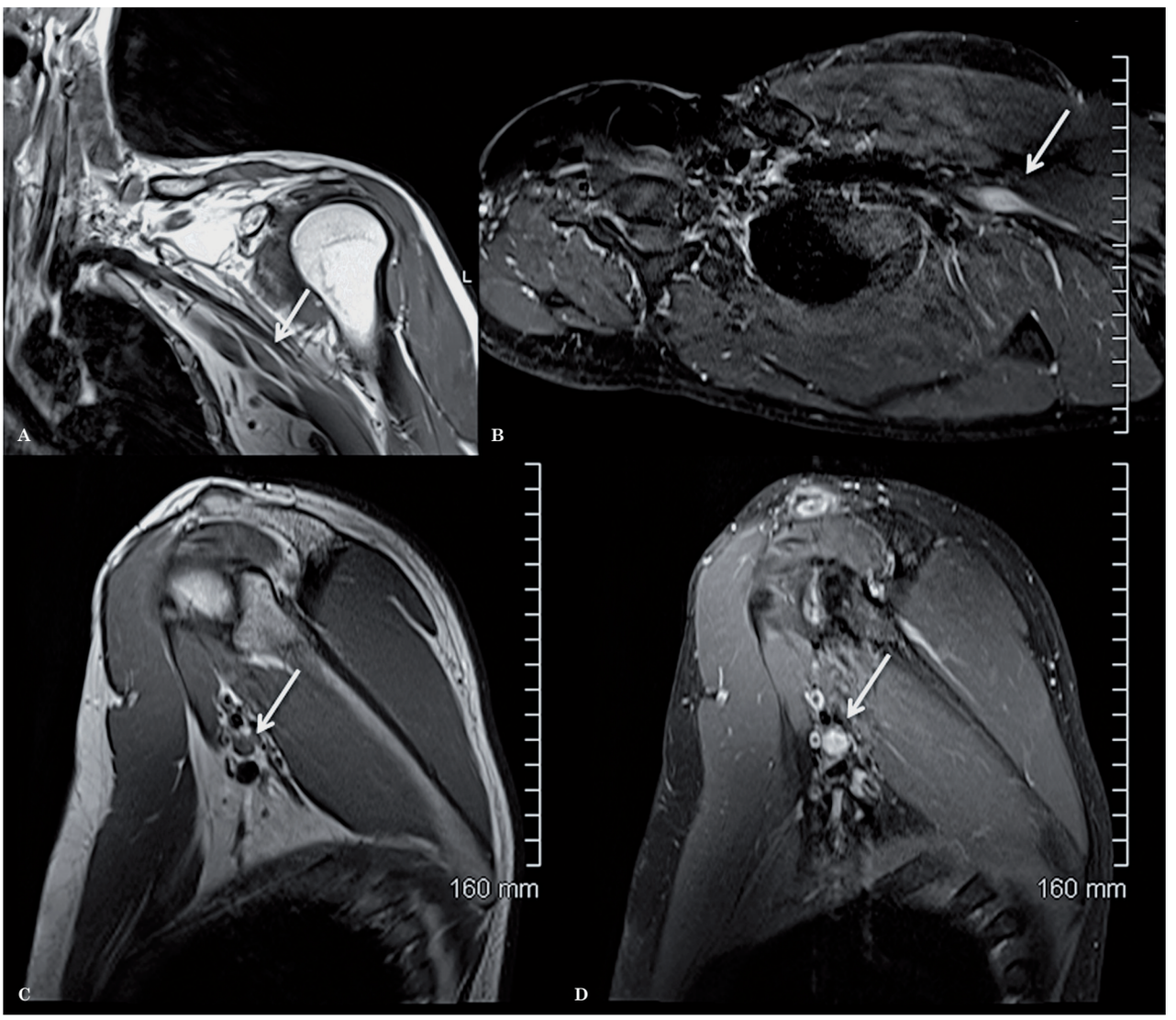

Figure 12 MRI of left brachial plexus using the modified technique, in 2011, as a follow up study for ulnar neuropathy. Coronal oblique T1 (A), axial oblique T1 post-contrast with fat saturation (B), sagittal T1 (C) and sagittal T1-weighted sequence post-contrast with fat saturation (D) show a focal well-defined enhancing mass lesion along the proximal branches of the left brachial plexus, likely consistent with a schwannoma.

the need for an in FOV saturation band. Figures 6 through 8 demonstrate the planning modifications between the conventional technique and the modified technique we have been using at our institution since 2007. This protocol can be easily used in 1.5 and 3 Tesla magnets.

Result

By modifying the technique, we were able to decrease the regular scan time by 11 minutes and ten seconds, due to the fact that fewer slices are needed per sequence since we now know exactly where the brachial plexus is located. In addition, we removed the coronal and sagittal T2W sequences from the conventional protocol and replaced them with a coronal STIR. If necessary, the T1 axial oblique sequence could be removed as well, further decreasing the scanning time. Table 1 shows the scan time difference for each sequence between the conventional and the modified techniques.

As an added bonus and given the fact that we are obtaining the images parallel to the segments of the brachial plexus, we are now able

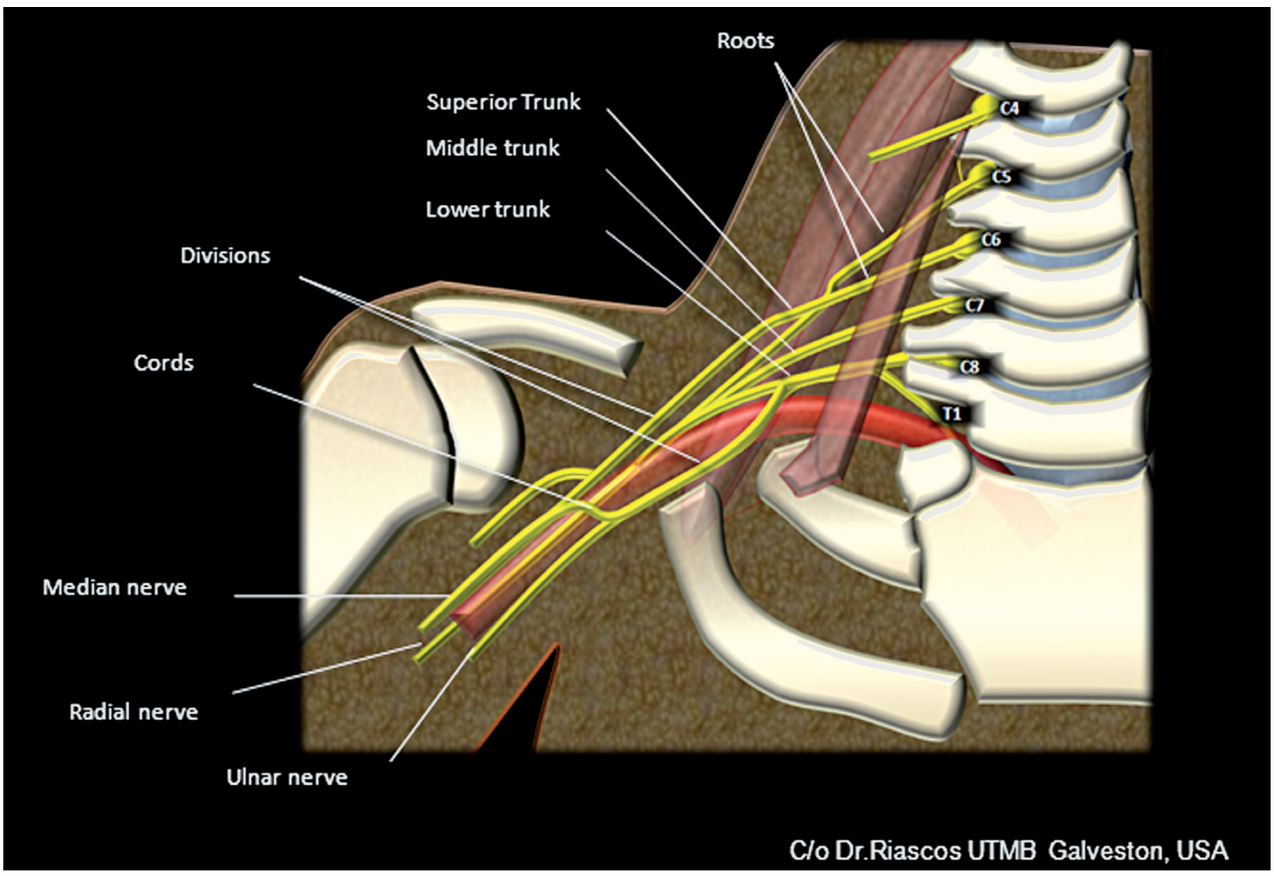

Figure 13 Cartoon of the anatomy of the brachial plexus.

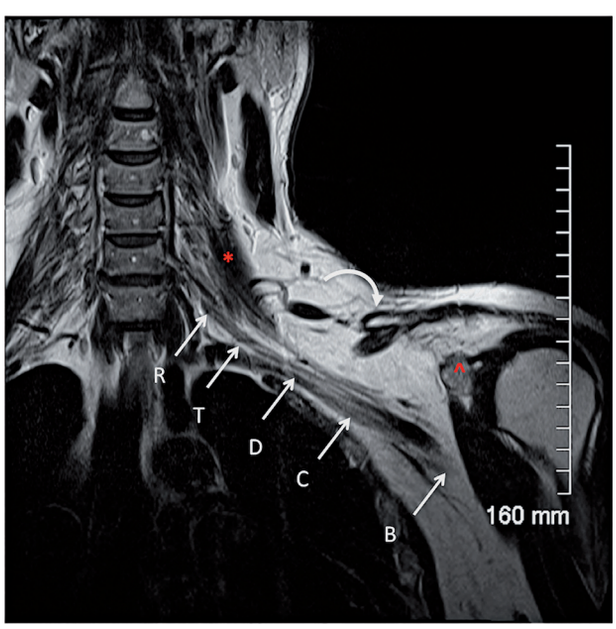

Figure 14 Normal anatomy. A coronal oblique T2W sequence shows the different segments of the brachial plexus. The roots (R) are located medial and within the scalene triangle; the middle scalene muscle (*) demarcates the lateral border of the scalene triangle. The trunks (T) are visualized at the lateral border of the scalene triangle, the divisions (D) between the first rib and the clavicle (curved arrow) and the cords (C) and the terminal branches (B) on both sides of the coracoid process of the scapula (^).

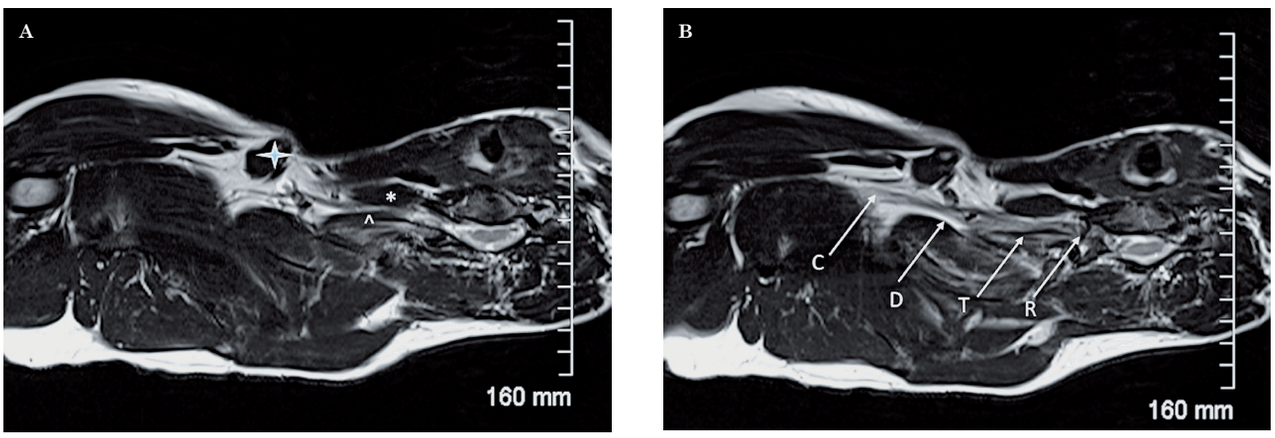

Figure 15 Normal anatomy. An axial oblique T2W sequence shows important anatomical landmarks. A) the anterior scalene muscle (*), the middle scalene muscle (^) and the clavicle (arrowhead) are identified. B) It is possible to appreciate how the roots (R) exit the neuroforamina and join within the scalene triangle to form the trunks (T). The divisions (D) are located behind the clavicle and become the cords (C) distally.

Figure 16 Normal anatomy. Sagittal T1W sequence of the brachial plexus. A) The image shows the 3 scalene muscles (A: anterior, M: middle, P: posterior) and the roots (arrowhead) within the scalene triangle. B) A more lateral image shows the anterosuperior position of the divisions (arrowhead) with respect to the first rib (curved arrow). The subclavian vein (o) is located anterior to the subclavian artery (*) at this level. C) At the level of the axilla and coracoid process (arrow), the proximal branches surround the subclavian artery (*) which is localized above the subclavian vein (o).

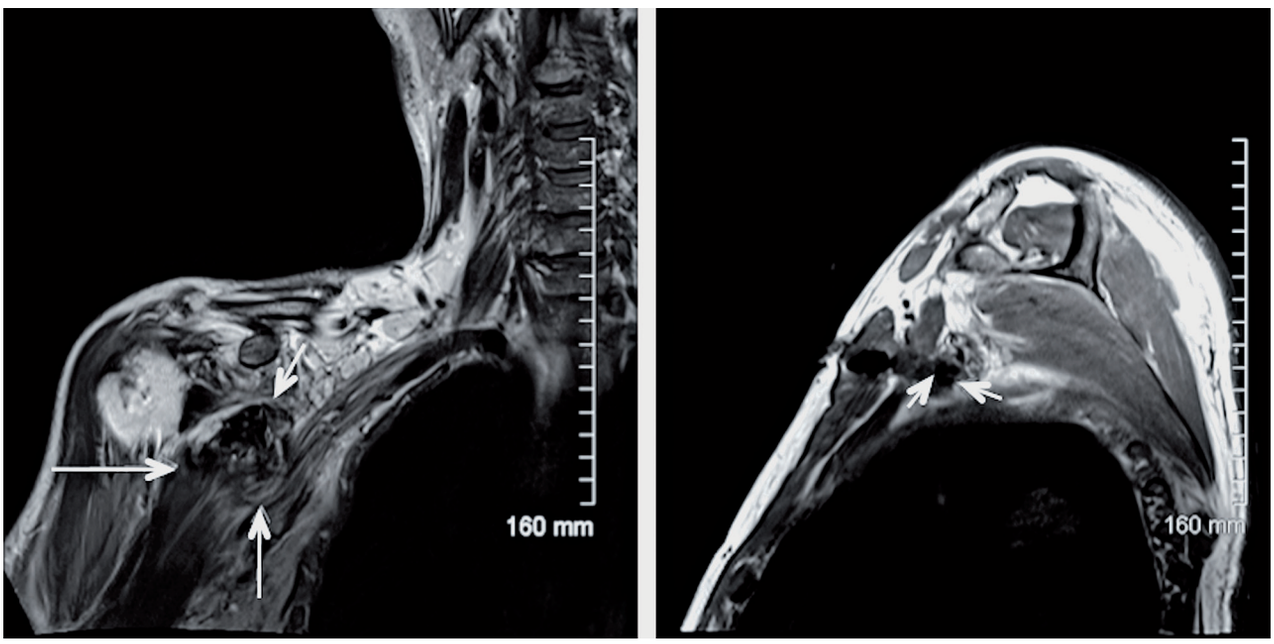

Figure 17 Coronal T2 (A) and sagittal T1W sequences (B) show a large post-traumatic hematoma (arrows) causing extrinsic compression on the divisions and cords of the right brachial plexus in a patient with penetrating injury with a knife.

to assess the plexus in a continuous fashion from the roots to the proximal branches in only one to three slices (Figures 9 and 10).

We illustrate the benefit of this modified technique with an example of a patient with a lesion in the proximal branches of the left brachial plexus that was clinically suspected but missed on conventional brachial plexus imaging for six consecutive years (Figure 11). Clinically, the patient had tingling, numbness and weakness in the left ulnar nerve distribution and the ulnar motor conduction studies revealed proximal conduction block near the axilla. The neurologist was suspecting a benign non-aggressive lesion of the ulnar nerve. A follow-up MRI was performed in 2011 using for the first time in this patient the modified technique for the study of the plexus which revealed a well-defined enhancing mass lesion along one of the proximal branches of the brachial plexus, most likely consistent with a schwannoma (Figure 12).

Normal brachial plexus anatomy

The brachial plexus originates from the ventral rami of nerves C5-C8 and T1, with occasional contribution from the anterior rami of C4 and T2 giving rise to a pre-fixed and post-fixed brachial plexus respectively, as normal variants. The nerve roots join to form the three trunks within the scalene triangle between the anterior and middle scalene muscles. The ventral rami of the C5 and C6 nerve roots converge to form the upper trunk, the ventral ramus of C7 continues as the middle trunk and the ventral rami of C8 and T1 join to form the lower trunk. Just lateral to the scalene triangle, each trunk splits into two to give an anterior and posterior division for a total of six divisions. The anterior divisions provide innervation to the flexor muscles and the posterior divisions to the extensor muscles of the arm. At the level of the first rib, the divisions merge to form three cords. The anterior divisions of the upper and middle trunks join to form the lateral cord, the anterior division of the lower trunk forms the medial cord and the three posterior divisions join to form the posterior cord. The names of the cords originate from their position in relation to the subclavian/axillary arteries. At the lateral margin of the pectoralis minor muscle and below the anterior coracoid process of the scapula, the cords divide into five branches: the ulnar, median, musculocutaneous, radial and axillary nerves [1-4] (Figure 13).

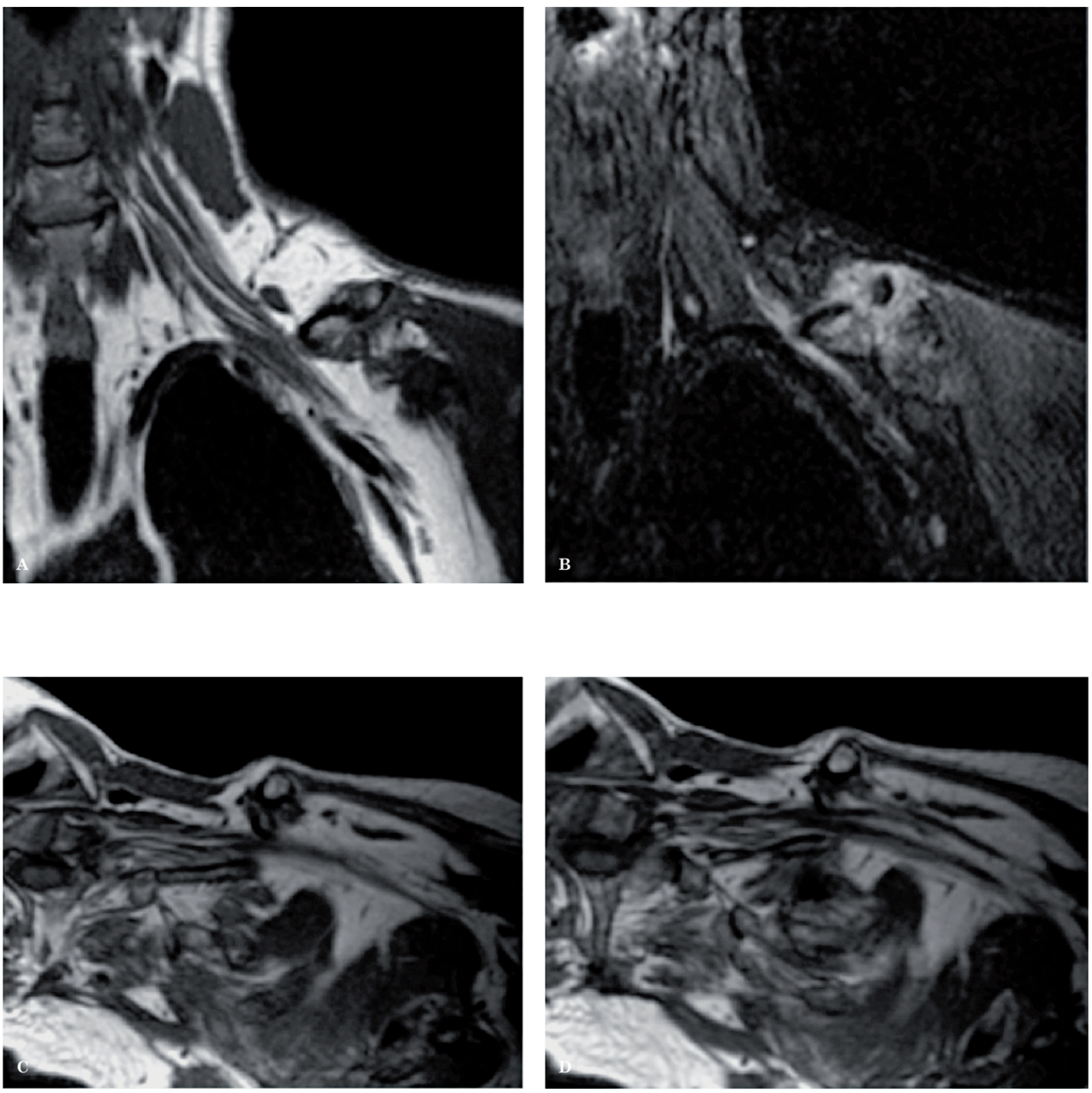

Figure 18 Fracture of the left clavicle with prominent callus formation exerting mass effect on the divisions of the brachial plexus. Coronal oblique T1 (A), coronal oblique STIR (B) and axial oblique T1W sequences (C,D). Note the increased signal intensity of the divisions in the STIR sequence secondary to inflammatory changes.

The roots, trunks, divisions, cords and branches of the brachial plexus appear as linear structures isointense to muscle and surrounded by fat in all the sequences. The roots are better seen in the axial plane while the remainder of the segments of the brachial plexus are better identified in the sagittal and coronal planes.

There are useful anatomical landmarks that help identify the different segments of the brachial plexus. The first one is the scalene triangle formed by the anterior and middle scalene muscles. The roots are located medial and within the triangle where they merge, the trunks are found immediately lateral to the tri-

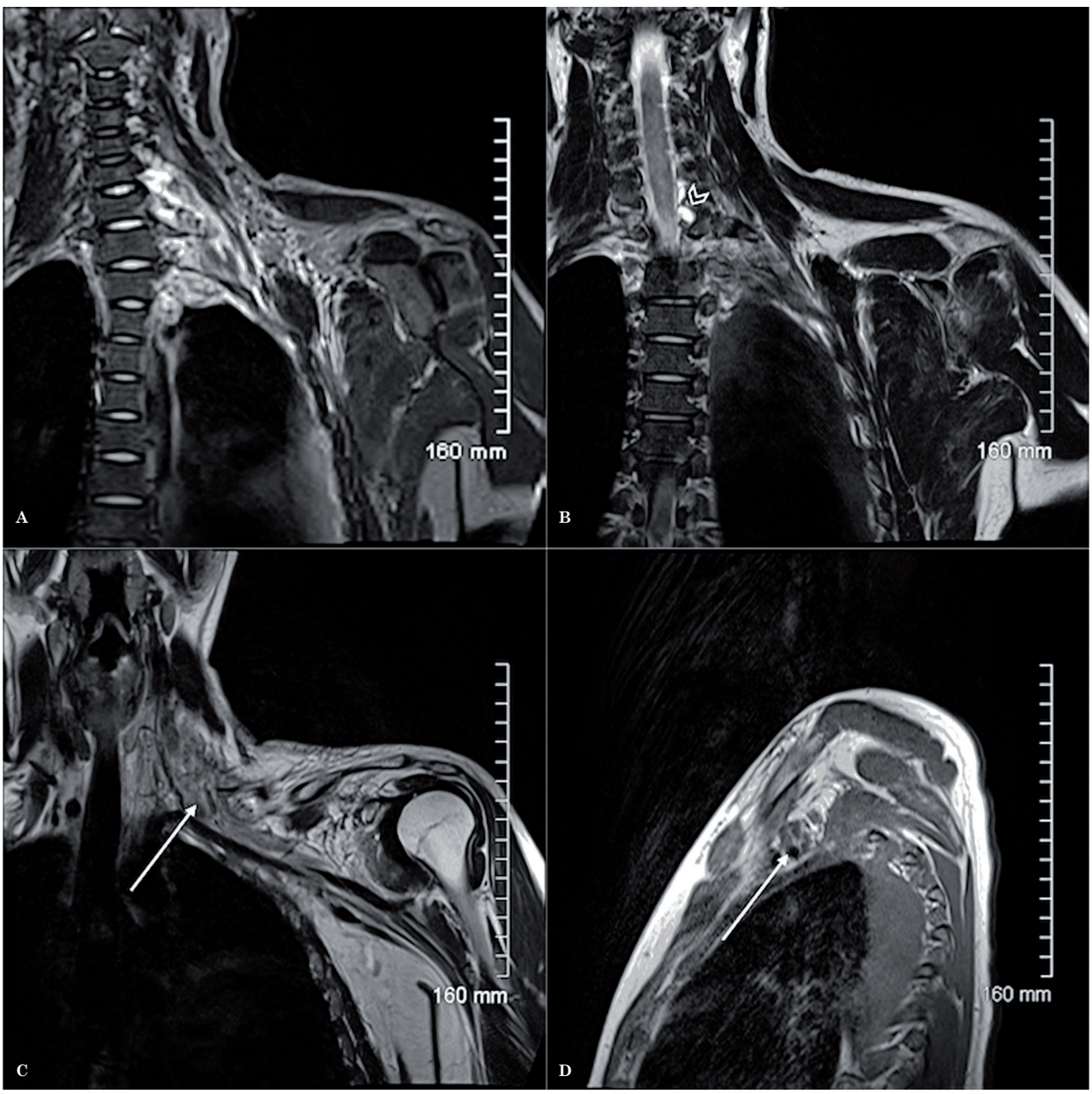

Figure 19 Trauma. Coronal oblique T2 (A,B), coronal oblique T1 (C) and sagittal T1W sequences (D) demonstrate thickening and increased T2 signal of the plexus (A,B) secondary to edema (arrows). The brachial plexus is ill-defined and there is distortion and stranding of the surrounding fat due to inflammatory changes. Two post-traumatic pseudomeningoceles (B) are identified at the level of C6-C7 and C7-T1 (arrowhead).

angle. The divisions are identified between the first rib and the clavicle; they merge to form the cords. The cords are completely formed at the level of the medial border of the coracoid process. The terminal branches are formed in the axilla, at the level of the lateral margin of the pectoralis minor muscle (Figures 14-16).

Pathology

The different pathological processes that can involve the brachial plexus may be adequately assessed with MRI. The modified technique described in this article facilitates the characterization of the diverse pathologies. We will dis-

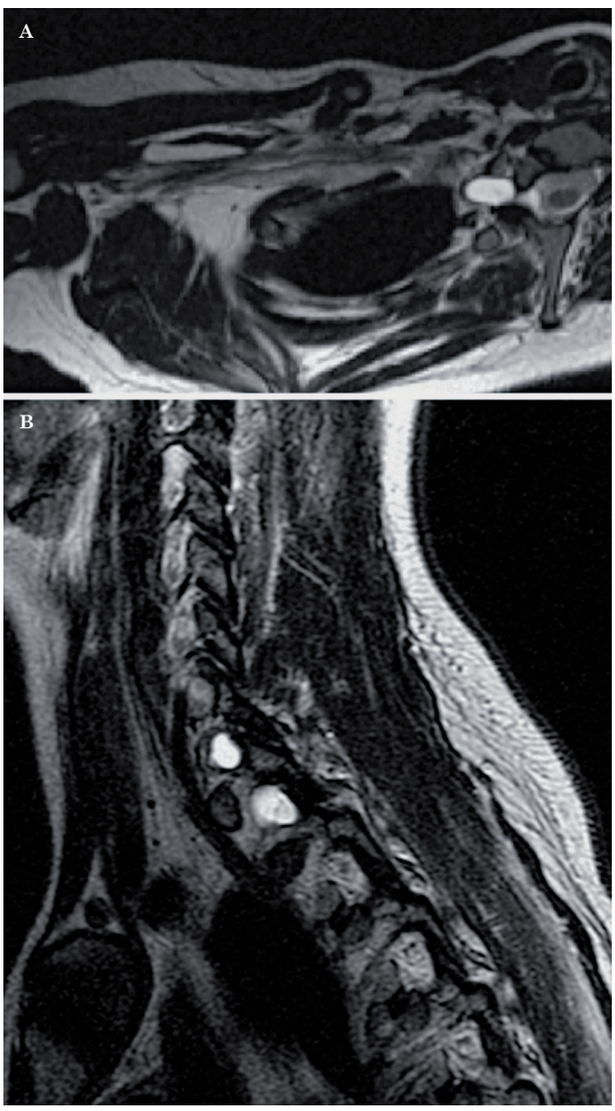

← Figure 20 Trauma. Axial oblique (A) and sagittal T2W sequences (B) in a different patient demonstrate post-traumatic pseudomeningoceles in 2 different levels. There are edematous changes in the trunks and divisions of the brachial plexus which are thickened and show increased signal intensity (A).

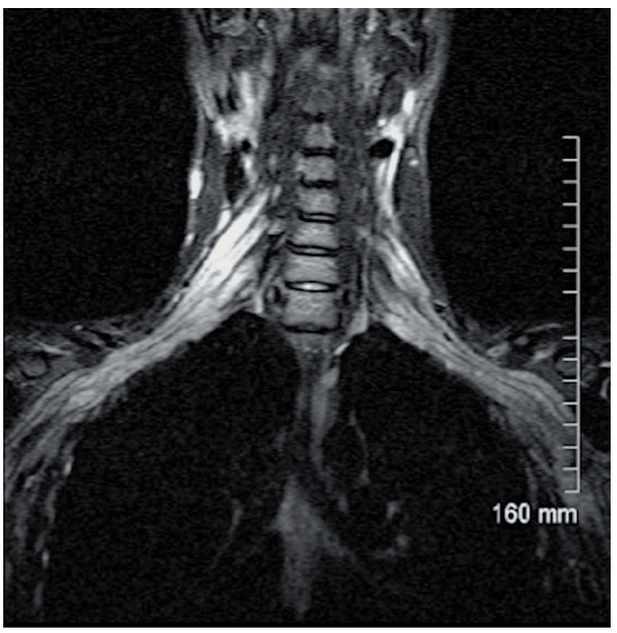

↑ Figure 21 CIDP. Coronal STIR sequence shows symmetric thickening and increased signal intensity of the bilateral brachial plexus.

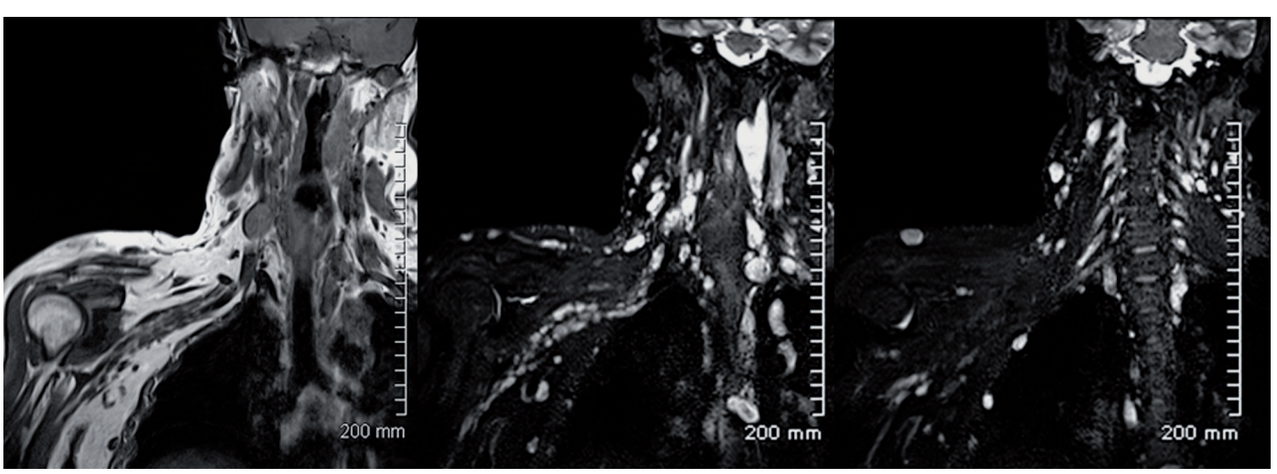

Figure 22 Multiple neurofibromas in a patient with Neurofibromatosis type 1. Coronal oblique T1 and coronal oblique STIR sequences show multiple ovoid masses along the right brachial plexus as well as in both paravertebral regions and in the subcutaneous tissues of the neck. These lesions are isointense to muscle in T1 and hyperintense in the STIR sequence.

Figure 23 Schwannoma. Coronal oblique T1 (A), sagittal T1 (B) and axial oblique T1W sequence post-contrast with fat saturation (C) show an ovoid mass (arrows), isointense to muscle in T1 with a peripheral "target sign" post-contrast enhancement involving the divisions of the left brachial plexus.

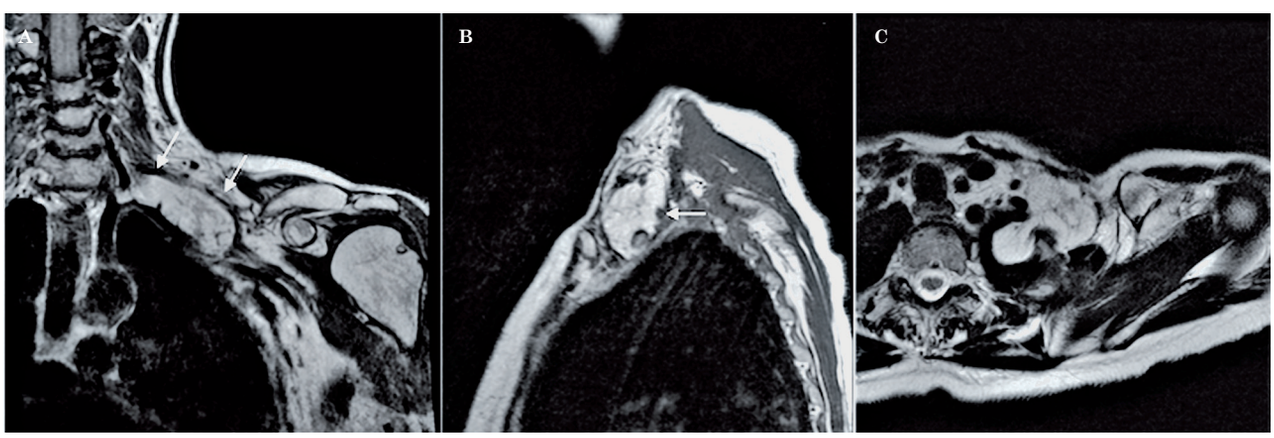

Figure 24 Lipoma. Coronal T1 (A), sagittal T1 (B) and axial T2W sequences (C) demonstrate a large lipoma within the scalene triangle with supraclavicular extension. The lipoma is splaying the roots and trunks (arrows) of the left brachial plexus.

cuss some examples of brachial plexus involvement in trauma, cancer, radiation fibrosis and inflammatory processes.

Trauma

Trauma is the most common brachial plexus pathology, found in more than 50% of cases [5]. It could be associated with nerve root avulsions without or with pseudomeningoceles and with compressive hematomas (Figure 17). Some of the traumatic injuries of the brachial plexus could be induced by clavicular fractures with or without callus formation (Figure 18) or by penetrating injuries [3]. Imaging findings on MRI will vary depending on which segment of the brachial plexus is involved and whether the injury is acute or chronic. Usually, in the setting of an acute injury, there is distortion of the brachial plexus with thickening and increased signal intensity of its segments in the T2 and STIR sequences, secondary to hemorrhage and neural edema.

Clinically, it is difficult to evaluate post-traumatic injuries of the brachial plexus. In patients with brachial plexus paralysis following trauma, it is important to differentiate between traumatic nerve root avulsions (generally with associated pseudomeningocele) (Figures 19 and 20) and distal lesions of the brachial plexus [3]. MRI is a fundamental tool to help differentiate preganglionic from postganglionic lesions, a differentiation that is key for determining the management of brachial plexus injury [6]. For preganglionic injury, the function of denervated muscles could be restored with nerve transfers. Postganglionic lesions may undergo microsurgical re-anastomosis and/or grafting or could be followed up conservatively [6,10].

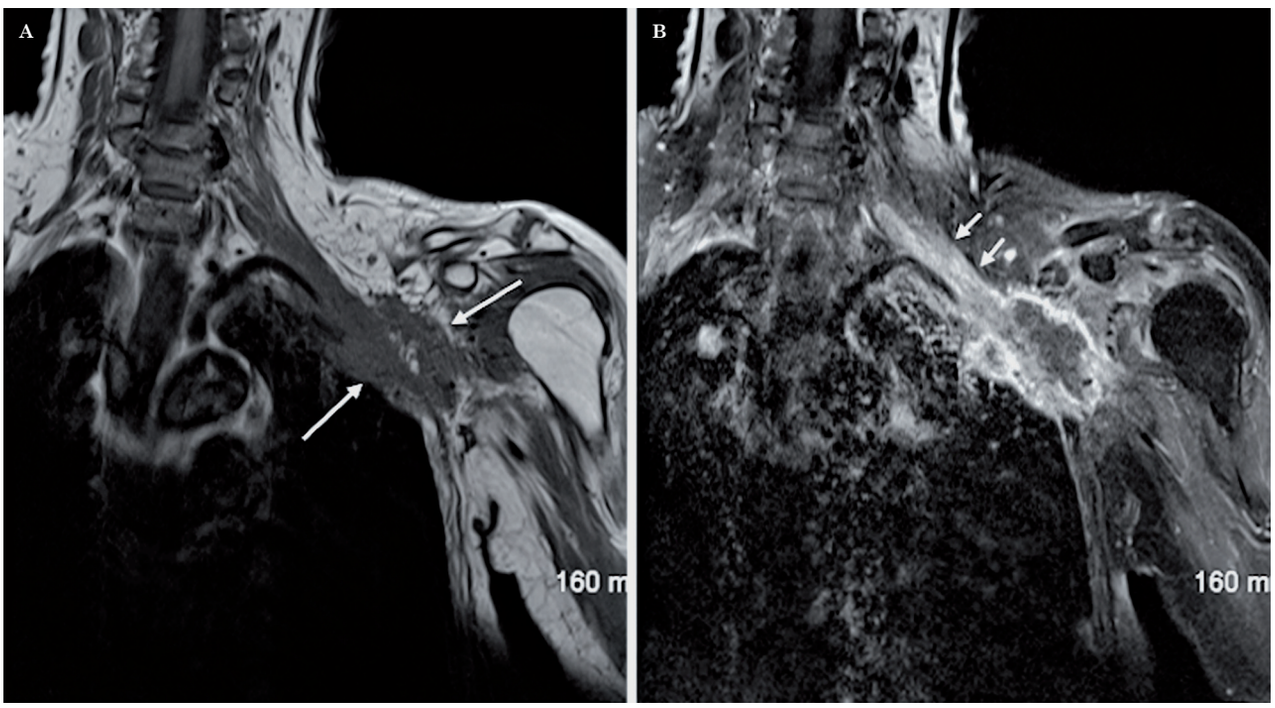

Figure 25 Lung cancer (Pancoast's tumor). Coronal oblique T1 (A) and coronal oblique T1W sequence post contrast with fat saturation (B) demonstrate a partially necrotic mass in the left lung apex, with peripheral enhancement (long arrows) which shows extension to the thoracic wall and invasion of the divisions and cords of the brachial plexus. In addition, there is malignant involvement of the proximal segment of the brachial plexus with thickening and post-contrast enhancement of the roots and trunks (short arrows).

Chronic Inflammatory Demyelinating Polyneuropathy

Chronic inflammatory demyelinating polyneuropathy (CIDP) is an acquired immune-mediated inflammatory process of the peripheral nervous system. Clinically, CIDP is characterized by symmetrical weakness in both proximal and distal muscles that progressively increases for more than two months, which differentiates this entity from Guillain-Barré syndrome, given the latter is self-limited [7]. This entity is associated with altered sensation, absent or diminished tendon reflexes, an elevated protein level in cerebrospinal fluid (CSF), demyelinating nerve-conduction studies and signs of demyelination in nerve-biopsy specimens [7]. There is a focal and asymmetrical variant of CIDP known as Lewis-Sumner syndrome.

MR images show diffuse thickening and enhancement of the proximal nerve roots secondary to an acute inflammatory demyelinating process of the brachial plexus or the cauda equina. Irregular thickening and increased T2 signal intensity of the brachial plexus has also been described in approximately 50% of CIDP patients [7] (Figure 21). The differential diagnosis includes viral neuritis and hereditary hypertrophic neuropathies like Charcot-Marie-Tooth disease.

Tumors

Primary Tumors

Primary neoplasms of the brachial plexus are uncommon, but include both benign and malignant neurogenic tumors. Schwannomas and neurofibromas are the most common benign tumors of the brachial plexus [1-3,16]. Histologically, neurofibromas are unencapsulated lesions believed to arise from the nerve fascicles [8]. These lesions tend to be sporadic in two thirds of cases or can occur in patients with neurofibromatosis type 1 (NF1) [1]. These tumors tend to be multiple, with diffuse involvement of the brachial plexus in neurofibromatosis (Figure 22), however, the imaging characteristics of the solitary neurofibroma and the schwannoma are very similar and often indistinguish-

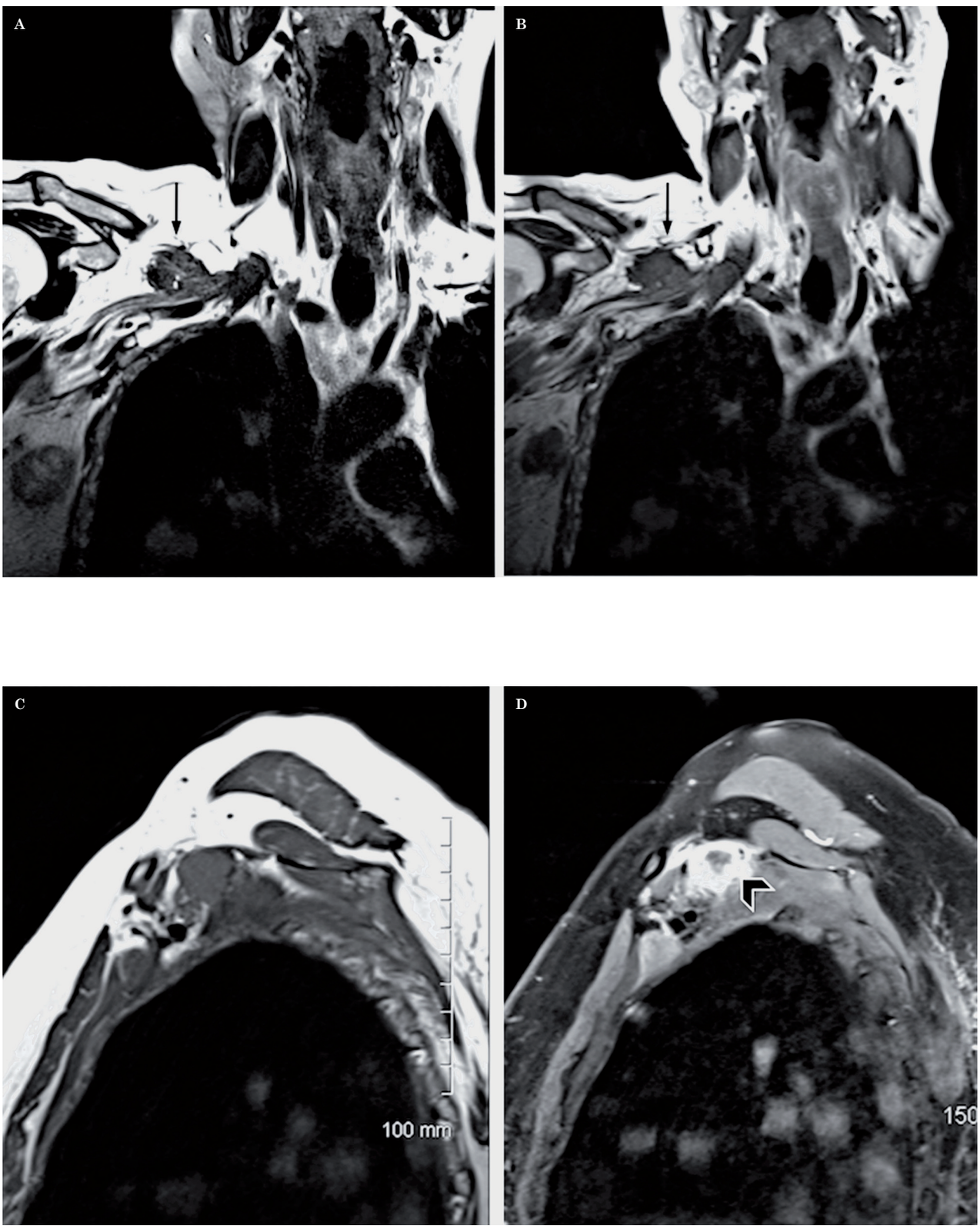

Figure 26 Metastasis from melanoma. Coronal oblique T2 (A), coronal oblique T1 (B), sagittal T1 (C) and sagittal T1W sequence post-contrast with fat saturation (D) show a partially necrotic mass with peripheral enhancement behind the clavicle and above the first rib (arrows in A and B and arrowhead in D) exerting mass effect on the divisions of the brachial plexus. Additional metastases are noted in the axillary region and in the right lung.

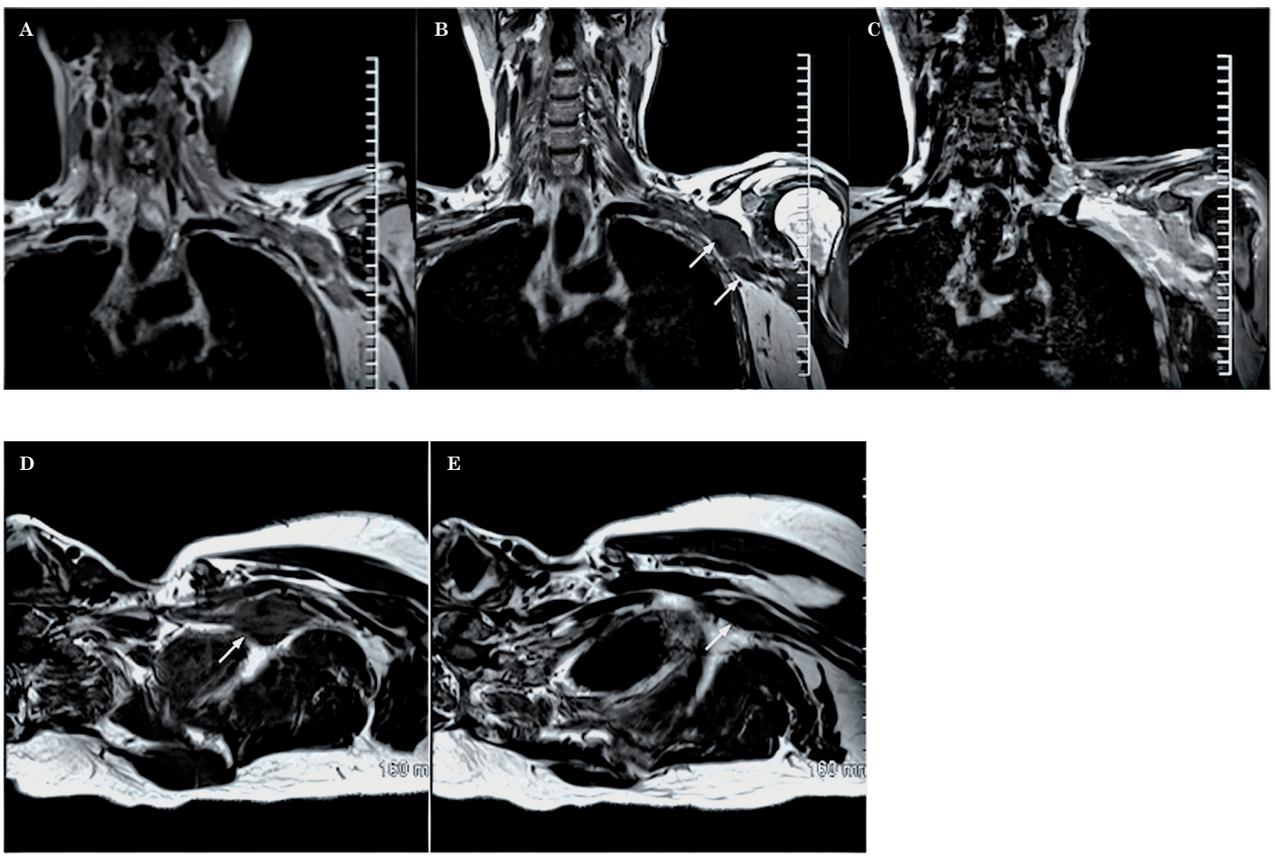

Figure 27 Neurolymphomatosis (diffuse large B-cell lymphoma). Coronal oblique T2 (A), coronal oblique T1 (B), coronal oblique T1 post-contrast with fat saturation (C) and axial oblique T1W sequences (D,E) demonstrate 2 masses (arrows) at the level of the divisions and cords of the left brachial plexus, which are isointense to muscle in T1, show minimal increased T2 signal as well as post-contrast enhancement. In addition, there is thickening and post-Gadolinium enhancement of the roots and trunks consistent with diffuse involvement of the plexus.

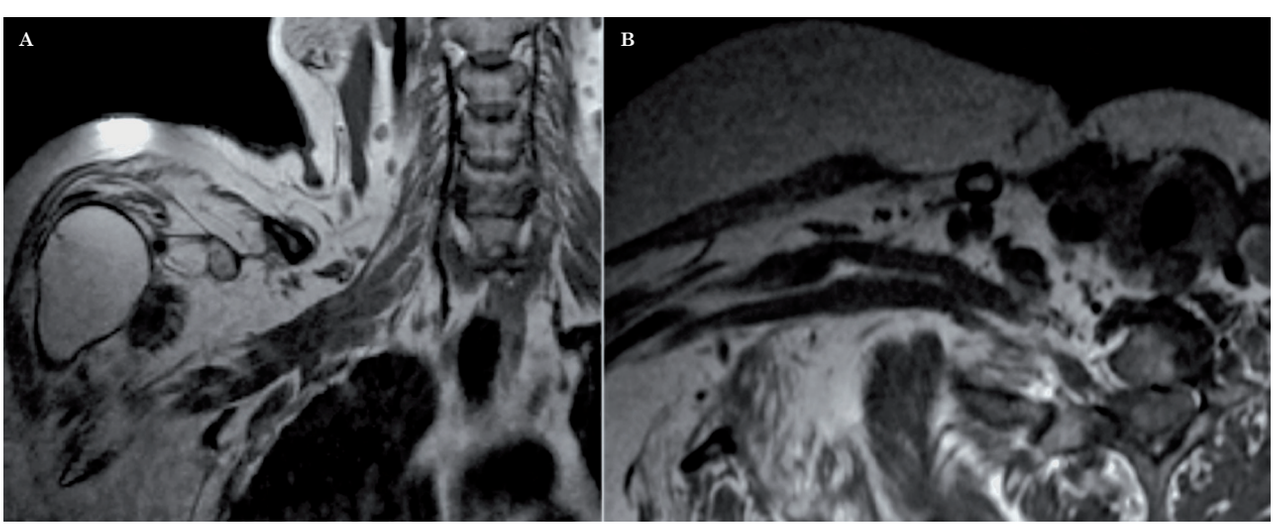

Figure 28 Radiation fibrosis. Coronal oblique T1 (A) and axial oblique T1 (B) show a marked diffuse thickening of the segments of the brachial plexus without evidence of a focal mass lesion in a patient with breast cancer and a history of radiotherapy.

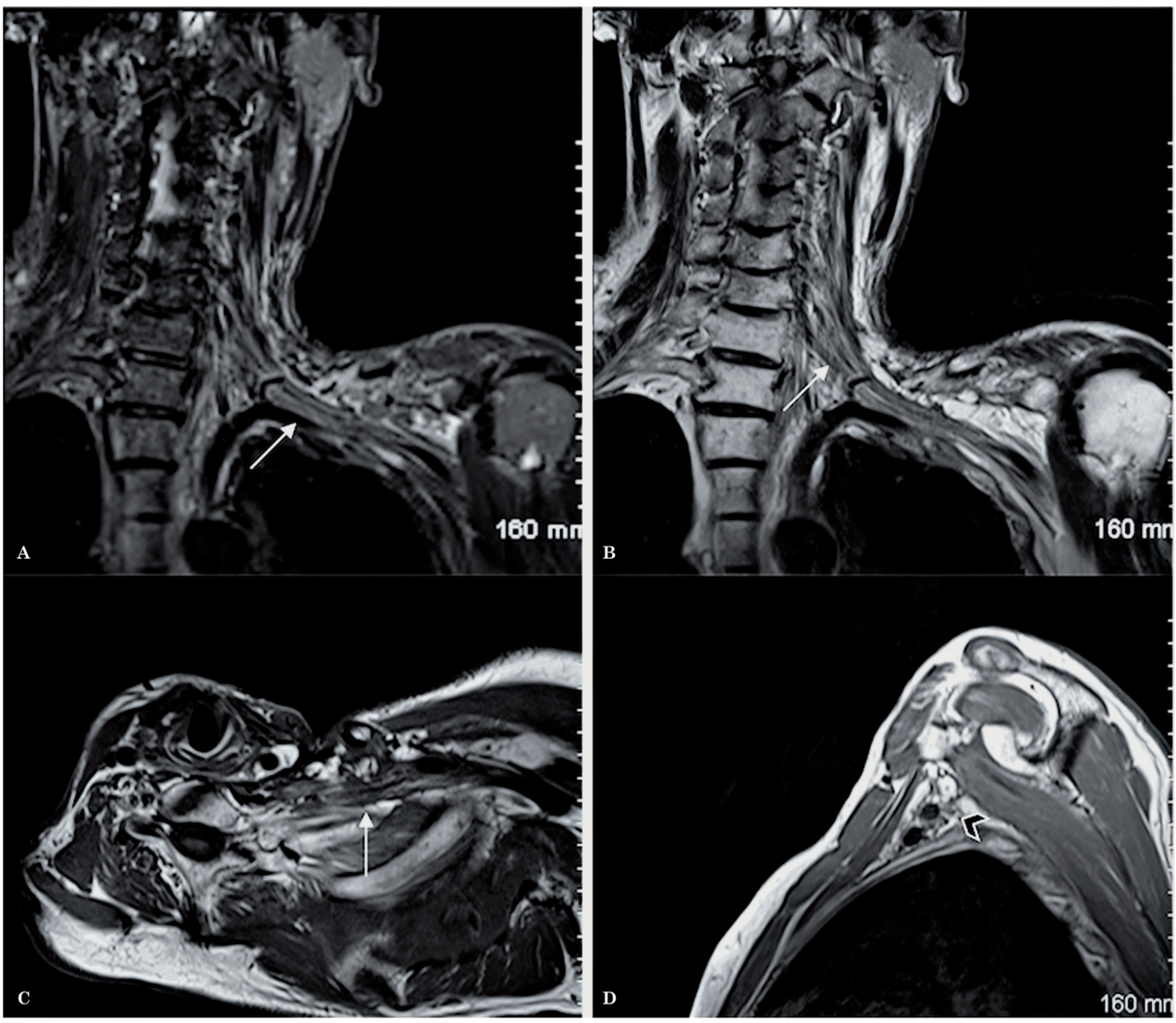

Figure 29 Radiation fibrosis in another patient. Coronal oblique STIR (A) coronal oblique T2 (B), axial oblique T1 (C) and sagittal T1W sequences (D) demonstrate a marked diffuse thickening of the segments of the brachial plexus as well. In addition, there is a significant distortion in the fat signal and architecture in the supraclavicular region and around the plexus in all the sequences. Note the low signal intensity of the segments of the plexus in the STIR and T2W sequences (A,B).

able. Schwannomas, on the other hand, originate from Schwann cells, they tend to grow eccentrically causing displacement of the nerve roots. Both neurofibromas and schwannomas are usually isointense to muscle in T1 and hyperintense in T2, STIR or fat saturated sequences [3]. In T2-weighted sequences, these lesions could have a central area of low signal or "target sign". Neurofibromas and schwannomas demonstrate avid enhancement after Gadolinium administration (Figure 23).

Other less common primary tumors that can involve the brachial plexus include lipomas, lymphangiomas and desmoid tumors [9]. Although the appearance of many benign processes is not specific, certain pathologies like a lipoma show imaging characteristics that suggest the exact diagnosis (Figure 24) [1].

Secondary Tumors

The brachial plexus can be involved by direct extension of a malignant tumor in its vicinity, arising from the lung (Pancoast's tumor) or soft tissues of the neck. It could also be involved by lymphoma or metastases, usually from breast

Table 1

Sequence	*Conventional Technique*	*Modified Technique*
Axial T1	7 min 25 s	3 min 59 s
Axial T2	8 min 03 s	3 min 54 s
Coronal T1	4 min 22 s	4 min 36 s
Coronal T2	4 min 44 s	3 min 54 s
Sagittal T1	9 min 16 s	6 min 17 s
Total scan time	33 min 50 s	22 min 40 s

or lung cancer [2,3]. These tumors are isointense to muscle in T1, hyperintense in T2 and in fat suppressed sequences and demonstrate post gadolinium enhancement.

Direct Invasion

The brachial plexus can be directly involved by primary tumors arising from the lung, bone or soft tissues of the neck, the supraclavicular fossa or the superior chest wall. Pancoast's tumor is an uncommon type of bronchogenic carcinoma that arises in the lung apex. This type of tumor can locally invade the ribs, vertebral bodies, subclavian vessels and the brachial plexus. MR images in the coronal and sagittal planes are very helpful to identify the tumor and its relationship with the adjacent structures (Figure 25) [17].

Metastasis

Metastatic disease to lymph nodes, bone or soft tissue can involve the brachial plexus and manifests as a focal mass or diffuse infiltration. As the lymphatic drainage of the breast is through the axillary apex, it is not uncommon to find brachial plexus invasion from recurrent or metastatic breast carcinoma. Metastatic involvement from lung cancer and melanoma may be seen as well (Figure 26).

Lymphoma

Occasionally, lymphoma and leukemia may involve the brachial plexus. These neoplasms are usually infiltrative and ill-defined, and demonstrate post gadolinium enhancement [10].

Neurolymphomatosis is an infrequent entity characterized by infiltration of the peripheral nervous system by malignant lymphoma cells. There is a selective involvement of cranial nerves and nerve roots in patients with primary central nervous system lymphoma or in patients with systemic lymphoma without lymphadenopathy [11]. This entity was originally described by Lhermitte and Trelles in 1934. The vast majority of neurolymphomatosis cases are due to diffuse large B-cell lymphoma when classified by the REAL or WHO systems [11].

The characteristic MR imaging findings include diffuse thickening of the roots, trunks and peripheral nerves, which show an increased T2 signal and marked post gadolinium enhancement. In addition to diffuse thickening, there may be focal masses arising from the endoneurium of individual nerve fascicles (Figure 27). Nodular thickening and post gadolinium enhancement, however, are not pathognomonic of this entity given these findings could also be identified in patients with acute and chronic inflammatory polyneuropathies or in peripheral nerve sheath tumors [12]. For that reason, it is important to interpret MR imaging studies in the clinical context of the patient [11]. Ga-67 scintigraphy tends to be very useful to confirm the diagnosis [13].

Radiation Fibrosis

Radiation to the axillary and supraclavicular regions can induce a progressive neuropathy secondary to perineural fibrosis and obliteration of the vasa nervorum [17]. This condition is more common after radiotherapy for breast cancer. Patients may develop a neuropathy months or years after radiotherapy, usually when the radiation dose is higher than 60 Gy [4,14].

MR findings include: diffuse thickening and variable enhancement of the brachial plexus without evidence of focal masses [14] as well as signal changes in the surrounding soft tissues

that demonstrate low signal intensity in the T1 and T2-weighted sequences [15]. There are certain imaging findings that are useful to help differentiate post-radiation changes from metastatic disease as follows: (a) stability of findings over time, on follow-up studies (b) the signal intensity of the brachial plexus in the T2-weighted sequence, which tends to be low in radiation fibrosis and high in tumoral and/or metastatic involvement [14]. There are few reports in the literature regarding the utility of gadolinium to differentiate radiation fibrosis from tumoral infiltration, but according to Wittenberg et al. the routine administration of contrast does not help to make that distinction given some degree of enhancement can be seen both in radiation fibrosis and in metastatic disease [1] (Figures 28 and 29).

Conclusion

Evaluation of the brachial plexus remains a challenge for the clinician and the radiologist. It is important for the radiologist to be familiar with the anatomy and imaging characteristics of the most common benign and malignant processes that can affect the brachial plexus. We believe that the modified technique to image the brachial plexus described in this article facilitates the understanding of the anatomy and the interpretation of the study.

References

1 Wittenberg KH, Adkins MC. MR imaging of nontraumatic brachial plexopathies: frequency and spectrum of findings. Radiographics. 2000; 20 (4): 1023-1032.
2 Blair DN, Rapoport S, Sostman HD, et al. Normal brachial plexus: MR imaging. Radiology. 1987; 165 (3): 763-767.
3 Van Es HW, Witkamp TD, Feldberg MAM. MRI of the brachial plexus and its region: Anatomy and pathology. Eur J Radiol. 1995; 5: 145-151.
4 Castillo M. Brachial and Lumbosacral Plexi. In: Mauricio Castillo. The Core Curriculum. Neuroradiology. 2nd ed. Philadelphia: Lippincott Williams and Wilkins; 2002. p. 463- 473.
5 Reede DL. MR imaging of the brachial plexus. Magn Reson Imaging Clin N Am. 1997: 5 (4): 897-906.
6 Takeharu Yoshikawa, MD, PhD, et al. Brachial plexus injury: clinical manifestations, conventional imaging findings, and the latest imaging techniques. Radiographics. 2006; 26 Suppl 1: S133-S143.
7 Köller H, Kieseier BC, Jander S, et al. Chronic inflammatory demyelinating polyneuropathy. N Engl J Med. 2005; 352 (13): 1343-1356.
8 England JD, Summer AJ. Nontraumatic brachial plexopathy. In: Wilkins RH, Rengachary SS, eds. Neurosurgery. 2nd ed. New York: McGraw-Hill, 1996. p. 3245-3250.
9 Lusk MD, Kline DG, Garcia CA. Tumors of the brachial plexus. Neurosurgery. 1987; 21 (4): 439-453.
10 Lury KM, Castillo M. Imaging the brachial plexus. Appl Radiol. 2004; 28-32.
11 Baehring JM, Damek D, Martin EC, et al. Neurolymphomatosis. Neuro Oncol. 2003; 5 (2): 104-115.
12 Byun WM, Park WK, Park BH, et al. Guillain-Barré syndrome: MR imaging findings of the spine in eight patients. Radiology. 1998; 208 (1): 137-141.
13 Ohta H. A case of non-Hodgkin's lymphoma infiltrating the brachial plexus detected by Ga-67 scintigraphy. Ann Nucl Med. 2002; 16 (4): 297-298.
14 Bowen BC, Verma A, Brandon AH, et al. Radiation-induced brachial plexopathy: MR and clinical findings. Am J Neuroradiol. 1996; 17(10): 1932-1936.
15 Wouter van Es H, Engelen AM, Witkamp TD, et al. Radiation-induced brachial plexopathy: MR imaging. Skeletal Radiol. 1997; 26 (5): 284-288.
16 Higgins CB, Steinbach LS. Magnetic resonance imaging of the body. New York: Raven Press, Ltd.; 1992. p. 443-460.
17 Posniak HV, Olson MC, Dudiak CM, et al. MR imaging of the brachial plexus. Am J Roentgenol. 1993; 161 (2): 373-379.

Carlos Torres, MD
Assistant Professor of Radiology
Program Director - Neuroradiology
University of Ottawa
The Ottawa Hospital Civic and General Campus
1053 Carling Ave
Ottawa, Ontario K1Y 4E9 Canada
Tel.: 613-798-5555 - Ext:12036
Fax: 613-761-4476
E-mail: catorres@toh.on.ca